

Synthesis and Characterization of Radial Oligothiophenes: A New Class of Thiophene-Based Conjugated Homologues

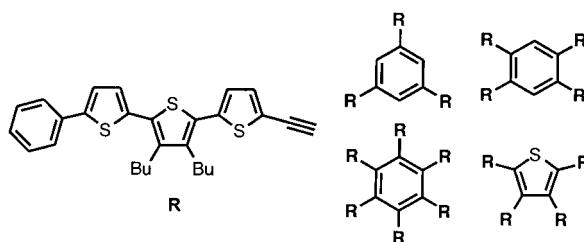
Ted M. Pappenfus and Kent R. Mann*

Department of Chemistry, University of Minnesota, Minneapolis, Minnesota 55455

mann@chem.umn.edu

Received June 3, 2002

ABSTRACT



A series of thiophene-based homologues with an aromatic core surrounded by terthiophene “arms” with acetylene linkages has been synthesized by using Sonogashira coupling methods. The homologues were investigated spectroscopically in solution and in the solid state. They display extended π -conjugation through the aromatic core that affects the strong emission and redox properties.

Conjugated organic oligomers and macromolecules continue to receive considerable attention for electronic devices such as field-effect transistors and light-emitting diodes.¹ For example, we recently reported a terthiophene-based quino-dimethane as an *n*-channel conductor in a thin-film transistor.² As part of an ongoing research project to create materials with favorable structural and optoelectronic properties, we now report the synthesis and electronic properties of a new class of radial oligothiophenes with oligophene “arms” around a central aromatic core attached with alkynyl linkages.

Vollhardt et al. first reported the synthesis of hexaethynylbenzene and its derivatives under high-temperature Sonogashira conditions.³ Also, tetraethynylthiophene has been reported by Whitesides and Neenan.⁴ Tour and co-workers

have thoroughly demonstrated the utility of triple bonds in a series of oligo(α -thiopheneethynyls) and studied their use in molecular scale electronic devices.⁵ Although similar “starlike” molecules and polymers have been prepared with thioether linkages⁶ and direct thiophene–aromatic core bonds,^{7–10} these systems are not anticipated to support extended π -conjugation through the core. The ethynyl

(1) (a) Torsi, L.; Dodabalapur, A.; Rothberg, L. J.; Fung, A. W. P.; Katz, H. E. *Science* **1996**, 272, 1462–1464. (b) Horowitz, G.; Delannoy, P.; Bouchriha, H.; Deloffre, F.; Fave, J. L.; Garnier, F.; Hajlaoui, R.; Heyman, M.; Kouki, F.; Valat, P.; Wintgens, V.; Yassar, A. *Adv. Mater.* **1994**, 6, 752–755.

(2) Pappenfus, T. M.; Chesterfield, R. J.; Frisbie, C. D.; Mann, K. R.; Casado, J.; Raff, J. D.; Miller, L. L. *J. Am. Chem. Soc.* **2002**, 124, 4184–4185.

(3) (a) Diercks, R.; Armstrong, J. C.; Boese, R.; Vollhardt, K. P. C. *Angew. Chem., Int. Ed. Engl.* **1986**, 36, 268–269. (b) Boese, R.; Green, J. R.; Mittendorf, J.; Mohler, D. L.; Vollhardt, K. P. C. *Angew. Chem., Int. Ed. Engl.* **1992**, 31, 1643–1645.

(4) Neenan, T. X.; Whitesides, G. M. *J. Org. Chem.* **1988**, 53, 2489–2496.

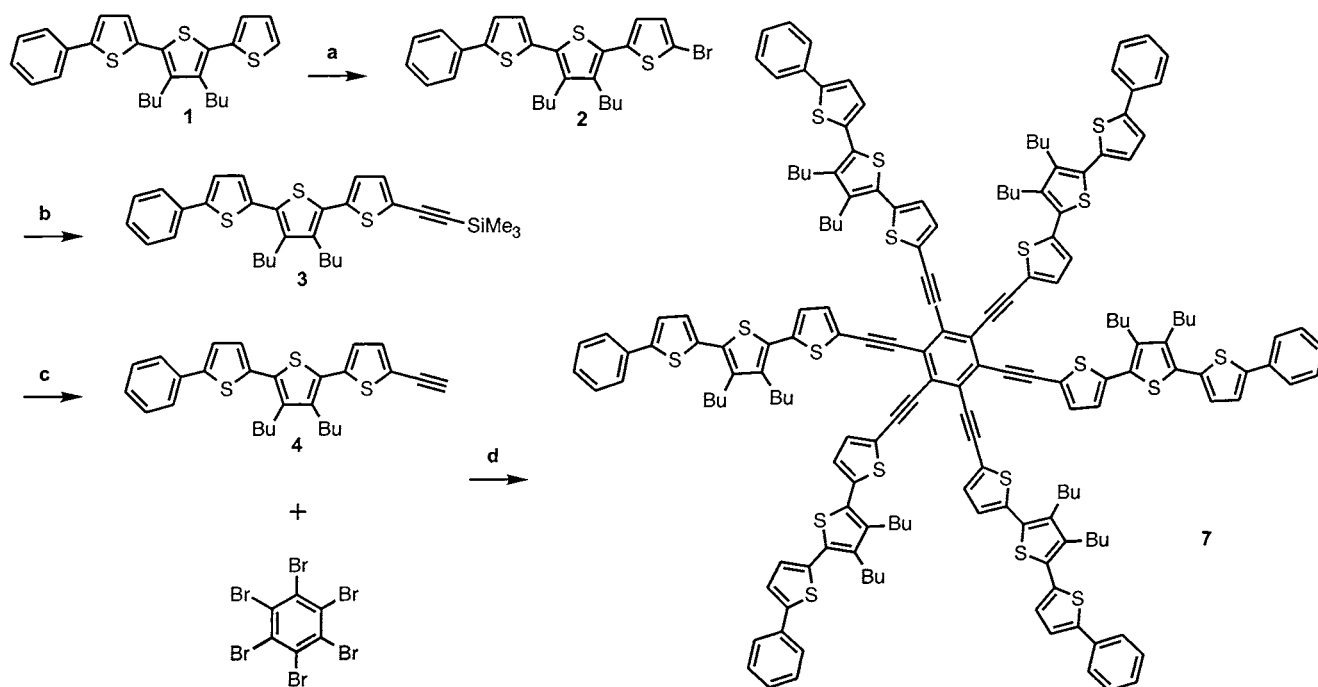
(5) (a) Pearson, D. L.; Jones, L., III; Schumm, J. S.; Tour, J. M. *Synth. Met.* **1997**, 84, 303–306. (b) Pearson, D. L.; Tour, J. M. *J. Org. Chem.* **1997**, 62, 1376–1387. (c) Wu, R.; Schumm, J. S.; Pearson, D. L.; Tour, J. M. *J. Org. Chem.* **1996**, 61, 6906–6921. (d) Tour, J. M. *Chem. Rev.* **1996**, 96, 537–553.

(6) Inoue, S.; Nishiguchi, S.; Murakami, S.; Aso, Y.; Otsubo, T.; Vill, V.; Mori, A.; Ujii, S. *J. Chem. Res. (S)* **1999**, 596–597.

(7) Geng, Y.; Fechtenkotter, A.; Mullen, K. *J. Mater. Chem.* **2001**, 11, 1634–1641.

(8) Wu, I.-Y.; Lin, J. T.; Tao, Y. T.; Balasubramaniam, E. *Adv. Mater.* **2000**, 12, 668–669.

(9) Kotha, S.; Chakraborty, K.; Brahmachary, E. *Synlett* **1999**, 10, 1621–1623.

Scheme 1^a

^a Reagents and conditions: (a) NBS, AcOH:CHCl₃, 0 °C; (b) (trimethylsilyl)acetylene, Pd(PPh₃)₂Cl₂, CuI, (iPr)₂NH, THF, rt; (c) K₂CO₃, CH₂Cl₂:MeOH, rt; (d) Pd(PPh₃)₂Cl₂, CuI, (iPr)₂NH, THF:toluene, reflux.

linkages between the oligothiophene arm and the benzene core enhance conjugation by allowing the arms and core to achieve coplanarity.

Radial oligothiophenes **5–8** were synthesized according to the general route in Scheme 1. Bromination of the phenyl-capped oligomer **1** with *N*-bromosuccinimide (NBS), fol-

Table 1. Physical Properties of Homologues 4–8

compound		absorption			emission			oligomer oxidation ^f
		λ_{max} , nm (ΔE , eV) ^a	ϵ (M ⁻¹ cm ⁻¹)	λ_{max} , nm (ΔE , eV) ^b	λ_{max} , nm (ΔE , eV) ^c	Φ^d	λ_{max} , nm (ΔE , eV) ^e	
4	RH	374 (3.32)	28,000	404 (3.07)	493 (2.51)	0.086	578 (2.15)	1.06 V ^g
5		400 (3.10)	120,000	433 (2.86)	520 (2.38)	0.21	583 (2.13)	0.93 V
6		417 (2.97)	140,000	456 (2.72)	576 (2.15)	0.34	661 (1.88)	0.87 V
7		458 (2.71)	180,000	499 (2.48)	615 (2.02)	0.20	690 (1.80)	---- ^h
8		402 (3.08)	110,000	434 (2.86)	570 (2.18)	0.21	661 (1.88)	0.88 V

^a Dichloromethane solutions. Reported values of ϵ are not corrected for overlap with other absorption bands. ^b Thin films. Reported values are uncorrected ATR values. ^c Dichloromethane solutions measured at room temperature with $\lambda_{\text{ex}} = 435.8$ nm. ^d Quantum yields measured relative to [Ru(bpy)₃](PF₆)₂ in acetonitrile, $\Phi = 0.062$.¹⁴ ^e Thin films on quartz slides. ^f Potential vs Ag/AgCl in a 0.1 M TBAPF₆/CH₂Cl₂ solution. All E° values, unless otherwise noted. ^g Irreversible process E_{pa} value provided. ^h Measurement precluded due to limited solubility.

lowed by a Sonogashira^{5,11} coupling with (trimethylsilyl)-acetylene afforded the silylated oligomer **3**. Protodesilylation with potassium carbonate gave the acetylide arm **4** in quantitative yield. To force complete substitution of the appropriate aromatic halide, 9, 20, and 36 molar equiv of **4** were added to produce **5**, **6**, and **7**, respectively, using Sonogashira coupling.

The electronic spectra of the arm and radial homologues were recorded in dichloromethane (Table 1); spectra of the benzene-core series are shown in Figure 1. The absorption

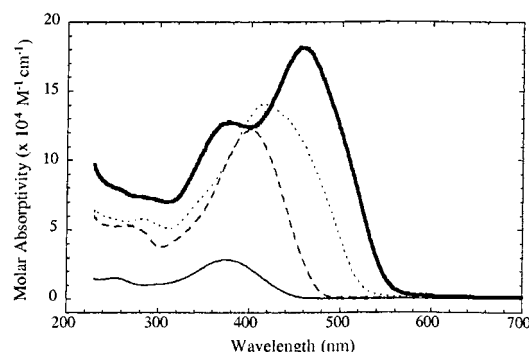


Figure 1. Electronic absorption spectra recorded in dichloromethane for **4** (—), **5** (---), **6** (···), and **7** (— ·).

maximum (λ_{max}) for the lowest π – π^* transition increases with the number of arms around the benzene core. The trend is consistent with a previously reported series of phenylethynyl-substituted benzene systems¹² and is evidence of extended π -conjugation through the benzene core. Homologue **8** with the thiophene core exhibits a maximum absorption at 402 nm and is substantially red-shifted relative to the arm (374 nm), again suggesting the formation of a delocalized π -system through the core.

Solid-state spectra of the homologues were also recorded. Figure 2 shows the electronic absorption spectrum of a thin film of **7** cast from a dichloromethane solution onto a cubic zirconia ATR crystal. The spectrum is red-shifted compared with the solution phase and exhibits low energy fine structure. Both qualities are characteristic of solid-state spectra of conjugated homologues and polymers.¹³ The large red-shift has generally been attributed to enhanced planarity of the molecule in the solid state. However, the origin of the fine structure is still debatable and will not be discussed here.

Figure 3 shows plots of the lowest energy transition vs the number of thiophene rings for the arm and benzene-core

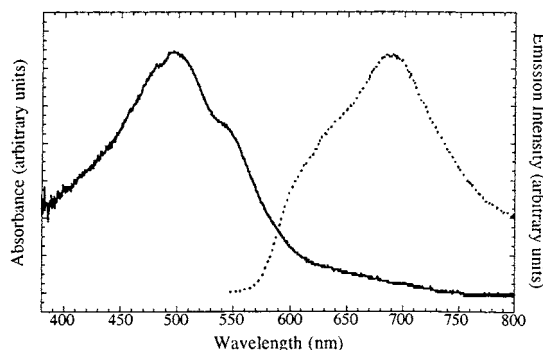


Figure 2. Electronic absorption spectrum (—) and emission spectrum (···) for thin films of **7**.

series for the solid and solution spectra. The series shows surprisingly good linearity. Typically, a plot of ΔE vs $1/n$ results in a linear relationship for π -conjugated oligomers and a saturation limit for ΔE vs n is reached for a given oligomer length.¹⁵ Clearly, this series of homologues is unique as no hint of a saturation limit for ΔE is evident as the number of thiophene rings is increased. To our knowledge, such a relationship is unprecedented in thiophene-based conjugated oligomers.

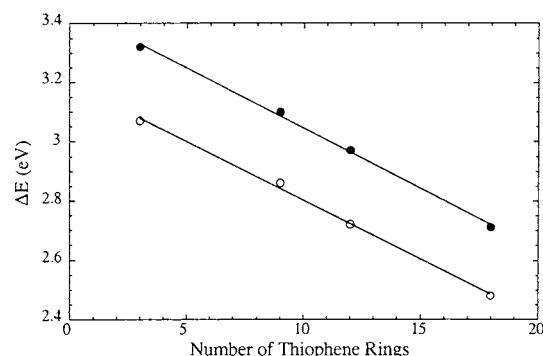


Figure 3. Energy (ΔE) of the lowest electronic transition for solution (●) and solid (○) for **4**–**7** vs the number of thiophene rings in the conjugated homologue.

The emissive properties of the homologues were also studied in solution and in the solid state (Table 1, Figures 2 and 4). As in the case for the absorption spectra, the emission spectra of the homologues display a distinct red-shift as the number of thiophene rings increases. The radial homologues exhibit good quantum efficiencies ($\geq 20\%$) in dichloromethane solution at room temperature (relative to the [Ru-

(10) (a) Cherioux, F.; Guyard, L. *Adv. Func. Mater.* **2001**, *11*, 305–309. (b) Cherioux, F.; Maillotte, H.; Audebert, P.; Zyss, J. *Chem. Commun.* **1999**, 2083–2084. (c) Cherioux, F.; Guyard, L.; Audebert, P. *Chem. Commun.* **1998**, 2225–2226.

(11) (a) Sonogashira, K.; Tohda, Y.; Hagihara, N. *Tetrahedron Lett.* **1975**, 4467. (b) Takahashi, S.; Hagihara, N.; Kuroyama, Y.; Sonogashira, K. *Synthesis* **1980**, 627.

(12) Kondo, K.; Yasuda, S.; Tohoru, S.; Miya, M. *J. Chem. Soc., Chem. Commun.* **1995**, 55–56.

(13) For example, see the following and references therein: Koren, A. B.; Curtis, M. D.; Kampf, J. W. *Chem. Mater.* **2000**, *12*, 1519–1522.

(14) Caspar, J. V.; Meyer, T. J. *J. Am. Chem. Soc.* **1983**, *105*, 5583–5590.

(15) (a) Jestin, I.; Frere, P.; Mercier, N.; Levillain, E.; Stievenard, D.; Roncali, J. *J. Am. Chem. Soc.* **1998**, *120*, 8150–8158. (b) Guay, J.; Kasai, P.; Diaz, A.; Wu, R.; Tour, J. M.; Dao, L. H. *Chem. Mater.* **1992**, *4*, 1097–1105.

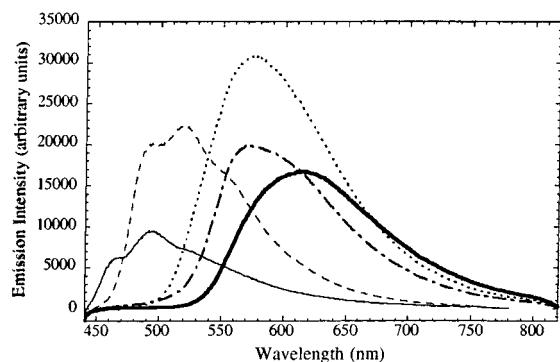


Figure 4. Emission spectra of **4** (—), **5** (---), **6** (···), **7** (— —), and **8** (- · -) in dichloromethane (relative intensity displayed).

(bpy)₃](PF₆)₂ ($\Phi = 0.062$) standard¹⁴). Emission spectra of solid films are red-shifted relative to the solution spectra, indicating the excited states of the thin films have greater conjugation lengths than in solution.

The redox properties of the homologues were investigated with cyclic voltammetry and Osteryoung square-wave voltammetry. The TMS-protected arm **3** displays two reversible one-electron oxidations with $E^{\circ'} = 1.00$ and 1.42 V. These two processes correspond to the sequential formation of a radical cation and dication. The protonated arm **4** exhibits irreversible oxidation processes at $E_{pa} = 1.06$ and 1.56 V and no stable oxidized species on the CV time scale are observed.

The radial homologues **5**, **6**, and **8** display stable oxidized species on the CV time scale. The redox behavior of **7** could not be determined due to limited solubility. The potential of the first oxidation for each homologue is listed in Table 1. Each homologue exhibits a lower first oxidation potential than the arm indicative of a more delocalized oxidized species. A representative cyclic voltammogram is provided for homologue **6** in Figure 5. Three distinct oxidation

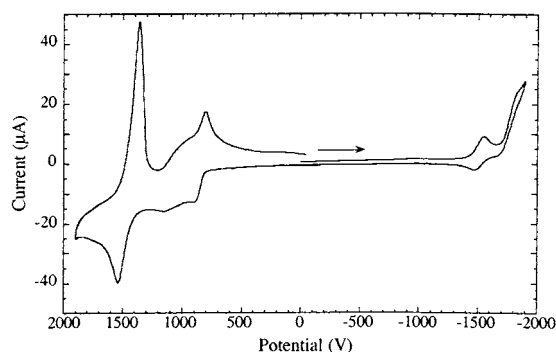


Figure 5. Cyclic voltammogram of **6** ($\nu = 100$ mV/s) in 0.1 M TBAPF₆/CH₂Cl₂ solution.

processes are observed for **6** at $E^{\circ'} = 0.87$, 1.06, and 1.51 V. The large current “spike” for the return of the third process is attributed to precipitation of the highly charged species generated in the third anodic process on the electrode surface. A reversible reduction ($E^{\circ'} = -1.49$ V) followed by an irreversible reduction ($E_{pc} = -1.81$ V) is also observed for **6**. The observation of reversible oxidations and reductions in thiophene-based homologues are rare and offer attractive prospects for device applications. These applications and further investigations of the redox behavior of these molecules will be reported soon.

Acknowledgment. This research was supported by the National Science Foundation under Grant CHE-9307837. We thank Daron Janzen for assistance with the emission data acquisition.

Supporting Information Available: Experimental procedures and absorption and emission spectra of the homologues. This material is available free of charge via the Internet at <http://pubs.acs.org>.

OL026292L